Analytical Biochemistry 627 (2021) 114210

Contents lists available at ScienceDirect

Analytical Biochemistry

journal homepage: www.elsevier.com/locate/yabio

A user's guide to multicolor flow cytometry panels for comprehensive immune profiling

Staffan Holmberg-Thyden [a,b], Kirsten Grønbæk [a,c,d], Anne Ortved Gang [a,c], Daniel El Fassi [a,c], Sine Reker Hadrup [b,*]

[a] Dept. of Hematology, Copenhagen University Hospital, Rigshospitalet, Denmark
[b] T-cells and Cancer, Experimental & Translational Immunology (XTI), Health Technology, Technical University of Denmark, Denmark
[c] Dept. of Clinical Medicine, University of Copenhagen, Denmark
[d] Biotech Research and Innovation Centre, BRIC, University of Copenhagen, Denmark

ARTICLE INFO

Keywords:
Flow cytometry
Immunology
Immune monitoring
Unsupervised clustering
Myelodysplastic syndrome

ABSTRACT

Multicolor flow cytometry is an essential tool for studying the immune system in health and disease, allowing users to extract longitudinal multiparametric data from patient samples. The process is complicated by substantial variation in performance between each flow cytometry instrument, and analytical errors are therefore common. Here, we present an approach to overcome such limitations by applying a systematic workflow for pairing colors to markers optimized for the equipment intended to run the experiments. The workflow is exemplified by the design of four comprehensive flow cytometry panels for patients with hematological cancer. Methods for quality control, titration of antibodies, compensation, and staining of cells for obtaining optimal results are also addressed. Finally, to handle the large amounts of data generated by multicolor flow cytometry, unsupervised clustering techniques are used to identify significant subpopulations not detected by conventional sequential gating.

1. Introduction

There are many occasions where it is important to examine the composition of immune cells in our body. For example, to correctly diagnose, characterize disease stages, or detect changes associated with disease or therapies. One way of achieving this is by flow cytometry, which measures scattered light from fluorescent-labeled antibodies that bind to specific cellular markers to determine frequencies of defined cell types [1,2]. The technology has been in use since the 1960s, and even though the general principles of the technology have not changed much, its application and complexity have vastly increased and now allows us to retrieve high dimensional data in parallel from a broad range of different cell types [3]. With the increased complexity, follows the need for a systematic approach for designing flow cytometry panels.

The performance of flow cytometers varies [4], even within models with similar laser- and filter configuration. To generate the most accurate results from flow cytometry experiments, the user must optimize panels to function with the specific machines intended to run the experiments. Thus, the choice of fluorescent labels for specific markers depends on both the instrument's capacity and setup and the antibody affinity and biological expression of the investigated markers. Adapting instruments to use existing panels, in order to perform comparable experiments at different laboratories, is also possible but requires rigorous control procedures to validate inter-assay variability, which might not be feasible for smaller or highly dynamic research environments.

We here describe a systematic approach to designing multicolor flow cytometry panels (Table 1) and provide a use case with examples of four comprehensive and complementary panels that cover some of the most important immune cell subtypes and their functional state in patients with cancer or autoimmune disorders. The workflow and principles described can be used to build and optimize research panels suitable for your own specific needs and available instruments.

1.1. Matching markers with colors

In order to build robust flow cytometry panels with as many colors as possible, while avoiding issues with spectral overlap, excessive compensation, or unfavorable loss of resolution, panels should be

* Corresponding author. Technical University of Denmark, Health technology, Kemitorvet, Building, 204 2800 Kgs. Lyngby, Denmark.
E-mail address: sirha@dtu.dk (S.R. Hadrup).

https://doi.org/10.1016/j.ab.2021.114210
Received 20 February 2021; Accepted 13 April 2021
Available online 24 May 2021

Table 1
Overview of flow cytometry panel design.

Panel design steps	
Choosing markers	Choose subpopulations of interest, e.g. effector and memory T cells. (Table 2) Define lineage markers for the subpopulations, e.g. CD3, CD8, CCR7, CD45RA. Add functional markers, e.g. PD-1, CTLA-4, CD69. (Fig. 2) Annotate the expected antigen density of the markers included, e.g. low, medium, high, very high. (Fig. 1) Investigate which subpopulations that co-express the same markers. (Fig. 2)
FACS machine	Know your machine. Which colors can be used with the current laser and filter setup, and can it be optimized? (Suppl. figure 1) Record single stained beads to create a spillover spread matrix (SSM). The calculated SSM show how colors overlap and quantifies their brightness, or stain index. (Fig. 1)
Match colors to markers	Place markers next to colors in the SSM in a spreadsheet, so that co-expressed markers are not represented by colors with large spectral overlap. (Fig. 1) Bright colors (with large stain index) are reserved for poorly expressed antigens and vice versa.
Test and optimize	Decide which clones to use for the antibodies, if multiple options are available. Test antibodies and titrate to the concentration generating the largest spread with lowest amount of background. (Fig. 3) Specific cell lines, or cell stimulation, might be needed to generate a positive signal when antibodies are tested. (Fig. 3) Stain cells with the full panel and evaluate. Make changes if necessary.
Using the panels	Create compensation with single stained beads or cells. Make sure the compensation generates satisfactory results on stained cells. It should be used for all your experiments intended for comparison. Be aware that application settings and PMT values should not change following compensation. Either use manual sequential gating for analyzing flow cytometry data (Figs. 4, 6, 8 and 10), or unsupervised clustering methods for exploratory purposes (Fig. 12).

designed by using a spillover spreading matrix (SSM) generated from the FACS machine intended to run the experiments (Fig. 1) [5]. The SSM is used to ensure that fluorochromes with significant spectral overlap do not associate with markers expressed on the same cell type unless the marker's expression (and thus its fluorescence intensity) with overlapping color is expected to be low. The staining indexes for the individual fluorochromes obtained from the SSM make sure that dim colors are used for highly expressed markers and vice versa. That way, colors with the best separation between positive and negative populations can be reserved for markers that are more difficult to detect due to low expression or poor antibody affinity while avoiding loss of resolution due to spectral overlap.

Determining the expected antigen density for markers included in the flow cytometry panel, or if they are co-expressed on a particular cell type, can be challenging. Researchers often rely on experience from previous experiments involving the marker in question, and their theoretical knowledge, for determining the expected antigen density. Reviewing the scientific literature to understand the dynamics of the involved markers is therefore paramount before designing experiments. Researchers can also find information on marker expression, antigen density, and antibody affinity for various clones among the technical description of antibodies at the manufacturers' websites. After colors have been matched with markers and antibody clones selected, each batch of purchased antibodies should be tested to verify their binding to antigens and titrated to determine which concentration generates the best possible separation while maintaining the lowest level of unspecific background signal. When antibodies have been successfully titrated, the full panels are tested on healthy donor or patient material, depending on sample availability. Maintaining an agile workflow is essential, so that initial smaller experiments can inform panel adjustments if necessary.

1.2. Compensation

Flow cytometry panels using multiple fluorochromes always require a compensation matrix to be calculated and applied before experiments can be run. If the spectral overlap is too high and the separation of positive and negative cell populations is low, the machine might not correctly distinguish overlapping colors from one another. High compensation values will then create a spreading error resulting in loss of resolution and poor sensitivity for detecting the affected markers.

Phenotype panel

			APC	APC-R700	APC-Cy7	BUV395	BUV737	BV421	BV480	BV650	BV711	BV786	FITC	PE	PE-CF594	PE-Cy5	PE-Cy7
flourochrome stain index	->		20	49	20	13	27	25	21	19	28	38	8	38	41	52	25
expression level	->		++	-	-	++++	+++	+++	++++	++	+	+	++++	++	++	+	++
marker	->		CCR7	-	NIR	CD4	CD28	CD45RA	CD8	CCR6	CXCR3	CD39	CD3	CCR4	PD-1	CD137	CD69
APC	CCR7		00	52	16	00	19	00	00	16	05	04	01	00	02	11	11
APC-R700	-		10	00	24	00	22	00	00	00	07	04	01	00	01	02	12
NIR	Viability		09	23	00	00	12	00	00	00	02	13	00	00	00	02	30
BUV395	CD4		00	00	00	00	00	00	00	00	00	00	03	04	00	00	00
BUV737	CD28		07	121	36	01	00	00	00	00	07	12	00	01	00	00	08
BV421	CD45RA		00	00	00	00	08	00	15	03	02	00	00	00	02	04	04
BV480	CD8		00	05	03	00	05	00	00	10	05	04	06	00	07	02	00
BV650	CCR6		25	45	09	00	37	01	00	00	26	18	00	01	07	07	09
BV711	CXCR3		09	164	29	00	106	01	00	06	00	50	01	00	00	02	13
BV786	CD39		00	14	22	00	25	01	00	02	04	00	01	00	00	00	21
FITC	CD3		01	02	00	00	00	00	04	00	00	00	00	02	02	01	01
PE	CCR4		04	04	00	00	03	00	00	04	03	01	04	00	33	07	08
PE-CF594	PD-1		11	10	02	00	08	00	00	06	07	03	01	08	00	18	16
PE-Cy5	CD137		121	69	19	00	33	00	00	28	29	08	02	09	06	00	44
PE-Cy7	CD69		00	04	14	00	08	00	00	00	00	12	01	05	04	01	00

		exp. level:	stain index:
APC	CCR7	++	20
APC-R700	-	-	49
NIR	Viability	-	20
BUV395	CD4	++++	13
BUV737	CD28	+++	27
BV421	CD45RA	+++	25
BV480	CD8	++++	21
BV650	CCR6	++	19
BV711	CXCR3	+	28
BV786	CD39	+	38
FITC	CD3	++++	8
PE	CCR4	++	38
PE-CF594	PD-1	++	41
PE-Cy5	CD137	+	52
PE-Cy7	CD69	++	25

Fig. 1. Example of panel design using a SSM. Stain index of the fluorochromes, obtained when creating the SSM, is plotted together with the expression level of the markers of interest. Markers can then be moved around to visualize how panel changes will affect the resolution of a marker, if two fluorochromes are attached to the same cell. High numbers in the SSM indicate high degree of spectral overlap between two colors, while a high stain index for a fluorochrome indicate a bright color that might be suitable for a poorly expressed marker. (For interpretation of the references to color in this figure legend, the reader is referred to the Web version of this article.)

Compensation is most commonly done by making single stained control beads for each of the antibodies used and acquiring them one by one in the FACS machine. For all tandem dyes (such as BV650 or PE-Cy5) the same antibody batch should be used for compensation measures, as will be used for your planned experiment, as variations in the conjugation between the covalently bound fluorescent molecules can affect the spectral properties. For the non-tandem dyes (e.g., PE, APC, or BV421), an antibody with the same fluorochrome can be used for compensation.

Before acquiring the unstained negative control and single stained controls, photomultiplier tube (PMT) values, or voltages, should be set for the detectors assigned to the fluorochromes used. These values are often automatically optimized when baseline settings are determined but should be confirmed during compensation. An optimal PMT value is the minimum value required to generate the largest separation between negative and positive populations. Low values reduce detection of dim antigens, while too high values can push positive signals off scale and increase the spectral overlap among detection channels. An effective way to ensure the optimal voltage is to quickly run through all single stained controls while increasing the PMT values until the largest separation between negative and positive populations is reached. If the distance does not increase, then the PMT value is decreased until the lowest PMT value generating the largest separation is reached. Following PMT adjustment and acquisition of compensation controls, the compensation is calculated using available flow cytometry software, such as FACSdiva™ or FlowJo™. Settings on the machine must remain the same during compensation as for the later experiments.

1.3. Quality control

To reduce inter-experiment variability, which is a topic of frequent debate [6–9], the same compensation, PMT values, and application settings, can be applied to all experiments intended for comparison. It is also crucial to perform daily calibrations using beads with multiple spectral peaks, e.g., the Cytometer Setup and Tracking (CS&T) system in machines from Becton Dickinson (BD), and to rigorously clean and rinse the flow cell before each experiment. Stained capture beads, or well-known cell lines, can be included as quality controls for each experiment session to detect variations in spectral overlap or fluorescent intensity over time. It is also important to prepare pre-made batches of antibody mixes to reduce pre-analytic errors due to slight variations in antibody volumes. A way of reducing the risk of inter-experiment variation is to plan experiments so that as many samples as possible are stained and analyzed simultaneously and by the same person. However, one should be aware that splitting samples up in a non-randomized fashion, e.g., analyzing responding patients and non-responders in separate experiments can introduce significant bias. If experiments are to be performed at multiple laboratory sites, using more than one FACS machine, or if the experiments are performed in a regulated or clinical environment, then a strict validation process should take place in order to document that the assay precision is within 10–25% CV (coefficient of variation) [10].

2. Result

2.1. Use case – immune monitoring using flow cytometry

We designed multicolor flow cytometry panels to monitor patients with high risk myelodysplastic syndrome (MDS), a malignant disease of the bone marrow, treated with a novel immunotherapy drug. Relevant markers were identified to distinguish important immune cell subtypes and markers associated with increased immune activation and inhibition (Table 2). Using a SSM table generated on our BD LSR Fortessa™, the selected markers could be split between four panels, each with a distinct thematic purpose. Bright colors were matched with dim antigens, and colors with significant overlap were avoided for markers that were known to be co-expressed on the same cell types (Fig. 1).

Table 2
Overview of the four panels.

Phenotype/Activation			Treg/Inhibitory		
Description	Marker	Color	Description	Marker	Color
T lineage	CD3	FITC	T lineage	CD3	FITC
T lineage	CD4	BUV395	T lineage	CD4	BUV395
T lineage	CD8	BV480	T lineage	CD8	BV480
Memory/ Effector	CD45RA	BV421	Memory/ Effector	CD45RA	BV421
Memory/ Effector	CCR7	APC	Memory/ Effector	CCR7	APC
Co-stim (lineage)	CD28	BUV737	Treg lineage	CD25	BV711
Chemokine	CXCR3	BV711	Treg lineage	CD127	APC-R700
Th lineage	CCR4	PE	Exhaustion	CTLA4	PE-Cy5
Th lineage	CCR6	BV650	Exhaustion	TIM-3	PE-Cy7
Activation (early)	CD39	BV786	Exhaustion	LAG-3	BV650
Activation (early)	CD69	PE-Cy7	Exhaustion	PD-1	PE-CF594
Activation (later)	CD137	PE-Cy5	Treg lineage	FoxP3 **(IC)**	PE
Exhaustion	PD-1	PE-CF594	Proliferation	Ki67 **(IC)**	BV786
Viability	Live/ dead	Near-IR	Viability	Live/dead	Near-IR
Myeloid/Blast			**NK/NKT**		
Description	Marker	Color	Description	Marker	Color
T lineage	CD3	FITC	T lineage	CD3	FITC
B lineage	CD19	FITC	T lineage	CD4	BUV395
Blast cells	CD34	BV711	T lineage	CD8	BV480
Myeloid lineage	CD11b	PE-Cy7	B lineage	CD19	BV650
Myeloid lineage	CD33	BUV395	NK activation	CD45RO	BV786
Myeloid lineage	CD14	BV480	NK activation	CD45RA	BV421
Myeloid lineage	CD15	BV786	NK lineage	CD16	APC
Myeloid lineage	CD16	APC	NK lineage	CD56	PE-CF594
MHC class II	HLA-DR	BV421	NK activation	CD38	BUV737
mDC lineage	CD11c	PE	NK activation	CD69	PE-Cy7
pDC lineage	CD123	BV650	NK activation	CD107a	PE-Cy5
Exhaustion (tumor)	PD-L1	PE-CF594	NKT cells	CD1d tetramer	PE
Viability	Live/ dead	Near-IR	Viability	Live/dead	Near-IR

The first panel focuses on memory and effector subtypes of CD4 and CD8 cells and their expression of markers related to their activation state. The second panel examines inhibitory markers on CD4 and CD8 cells and the presence of regulatory T cells. The third was designed to determine the composition of myeloid cells, including MDSC, DC, monocytes, and $CD34^{+}$ hematopoietic stem cells. The fourth panel included markers for B cells, NK cells, NK T, cells and their activation status. In all panels, except for the myeloid one, we used a common backbone of CD3, CD4, and CD8 antibodies. See Fig. 2 for a schematic overview of the subpopulations investigated in each panel.

Each antibody was then stepwise titrated to the concentration generating the best separation between positive and negative populations and the lowest background signal. To ensure that antibodies were titrated on the correct type of immune cell, the cells were pre-stained with viability dye and lineage markers (CD3, CD16, CD56). Markers associated with immune activation or exhaustion (e.g., CD39, CD69, CD137, PD-1, CTLA-4, LAG-3, TIM-3) may require in vitro activation of the given cell types (here T cells) before staining to secure a positive signal. We stimulated peripheral blood mononuclear cells (PBMC) from healthy donors (HD) for two days with PHA-L (5 μl/ml) and then ran the titration experiments on both stimulated and non-

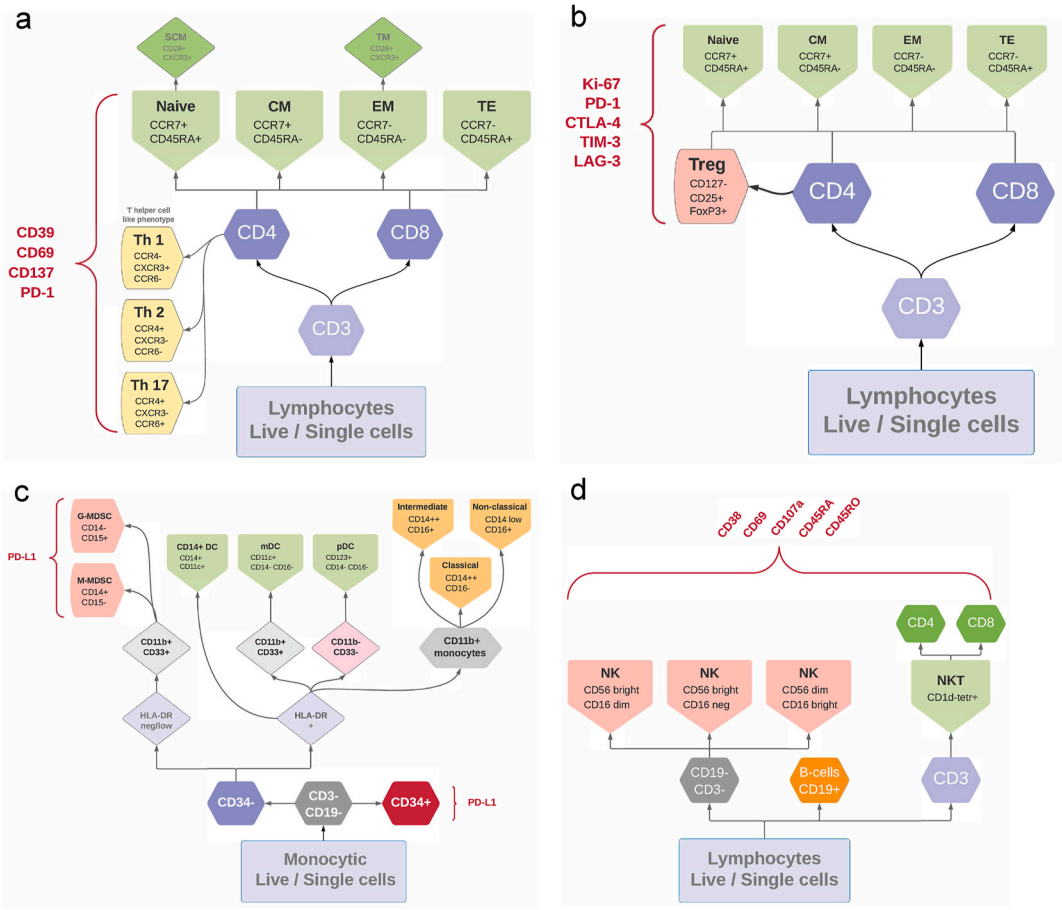

Fig. 2. Schematic overview of gating for (a) Phenotype panel, (b) Treg panel, (c) Myeloid panel, and (c) NK panel. Naive = Naive cell. CM = Central memory cell. EM = Effector memory cell. TE = Terminal effector cell. SCM = Memory stem cell. TM = Transient memory cell. Th = T helper cells. Treg = Regulatory T cell. G-MDSC = granulocytic myeloid derived suppressor cell. M-MDSC = Monocytic myeloid derived suppressor cell. mDC = Myeloid dendritic cell. pDC = plasmacytoid dendritic cell. NK = Natural killer cell. NKT = Natural killer T cell.

stimulated cells before selecting the appropriate antibody concentration (Fig. 3).

2.2. Phenotype panel

When working with cancer immunology, T cells are of major interest. CD8 T cells can recognize and kill cancerous cells by detecting altered peptide fragments bound to HLA class I molecules on cancer cells' surface [11]. CD4 T cells represent helper T cells (Th) and serve to orchestra the immune response.

CD8 and CD4 T cells are characterized into being memory or effector phenotype using CD45RA and CCR7. Terminal effector cells (TE) are $CD45RA^{+}$ $CCR7^{-}$, central memory (CM) $CD45RA^{-}$ $CCR7^{+}$, effector memory (EM) $CD45RA^{-}$ $CCR7^{-}$, while naive T cells are $CD45RA^{+}$ $CCR7^{+}$ [4]. CD8 cells can be further subdivided using CD28 and CXCR3 into a memory stem cell (SCM) population [12,13], that is $CD45RA^{+}$ $CCR7^{+}$ $CD28^{+}$ $CXCR3^{+}$, and a transient memory cell (TM) population that is $CD45RA^{-}$ $CCR7^{-}$ $CD28^{+}$ $CXCR3^{+}$ [12]. CD4 cells are also divided into their helper T cell class. In this case, Th1, Th2, and Th17 cells using CXCR3, CCR4, and CCR6. Th1 is $CXCR3^{+}$ $CCR4^{-}$ $CCR6^{-}$, Th2 $CXCR3^{-}$ $CCR4^{+}$ $CCR6^{-}$, and Th17 $CXCR3^{-}$ $CCR4^{+}$ $CCR6^{+}$ (Fig. 4) [14].

To evaluate the T cells' activation status, we included three markers associated with T cell activation (CD39, CD69, and CD137) and one inhibitory immune checkpoint (PD-1). CD39 is a marker expressed on the surface of activated T cells following recent antigen recognition. In the tumor microenvironment, these markers are reported to identify populations of tumor-specific CD4 and CD8 cells in cancer patients [15,16]. CD69, also a marker associated with activation of T cells and NK cells, that is detectable within 30–60 min after the cell has been activated, and then declines rapidly after 4–6 h [17,18]. CD137 is a molecule with costimulatory functions that is upregulated on T cells in response to activation, and it has also been described to identify tumor-reactive T cells in patients [19]. PD-1 is a classic immune checkpoint with inhibitory functions that can be blocked for therapeutic T cell activation in cancer immunotherapy. It gets upregulated when T cells are activated and can signal that a cell is reaching immune exhaustion [20].

A representative example of cells from bone marrow aspirates and PBMC from a patient with high-risk MDS, and PBMC from a HD, stained with the phenotype panel (Fig. 5), showed that the composition of memory and effector CD8 and CD4 T cells did not differ much between the bone marrow and peripheral blood samples in the MDS patient. Large differences were, however, seen when comparing the MDS samples to the healthy donor. In this example, the MDS patient had around 50% CD8 TE cells, compared to 11% in the HD, and 10% CD8 CM cells compared to 39% in the HD. T cells in the MDS patients' bone marrow expressed a higher level of activation markers, especially CD69, compared to T cells in the peripheral blood.

2.2.1. Characterization of antigen reactive T cells

Adaptations of the phenotype panel were developed to combine phenotyping with detection of specific antigen reactive T cells, either by detection of cytokine secretion following antigen stimulation or by staining T cell receptor specificities by using fluorescent-labeled MHC

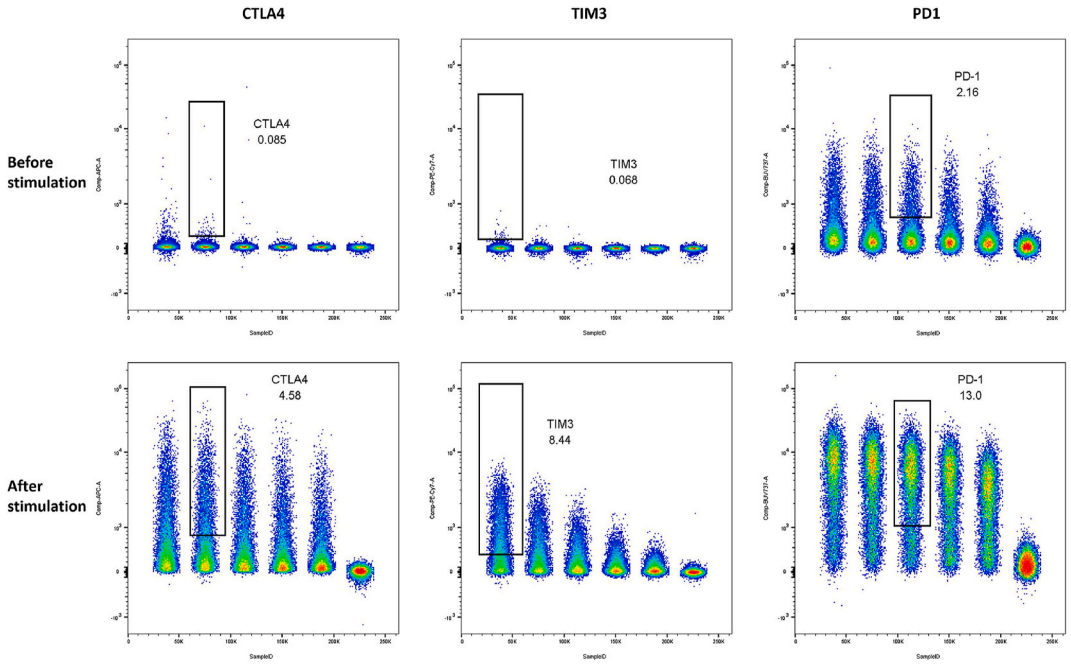

Fig. 3. Antibody titration experiment with decreasing antibody concentration for three markers associated with T cell exhaustion. Non-stimulated PBMC compared with PBMC stimulated with PHA-L for two days. CTLA-4 (left) and TIM-3 (middle) are here only stainable when the cells are activated, and stimulation is therefore necessary for choosing the right antibody concentration. PD-1 (right) expression is also increased when cells are stimulated, which facilitates selection of the correct antibody concentration.

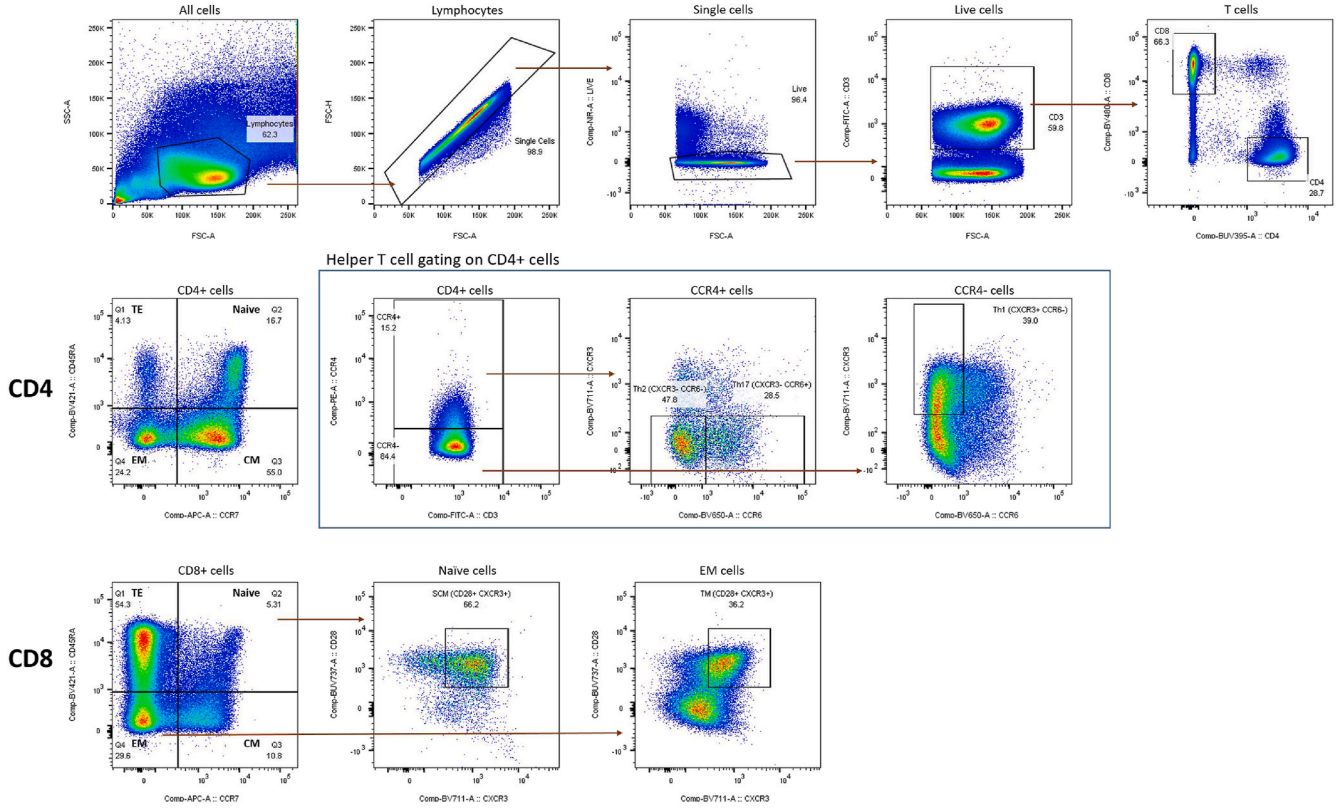

Fig. 4. Phenotype panel gated on PBMC from a patient with MDS. PD-1, CD39, CD69, and CD137 is measured on all subpopulations.

tetramers. To combine phenotyping with intracellular cytokine staining, the antibodies for CXCR3, CCR4, and CCR6 were replaced with antibodies binding IFN-γ, TNF-α, and the degranulation marker CD107a, and added following in-vitro stimulation with specific immunogenic peptides. When phenotyping was combined with MHC tetramer staining, peptides were loaded to tetramerized MHC molecules carrying a fluorescent label. The tetramers were then added to the cells in order to stain specific peptide-MHC reactive T cells.

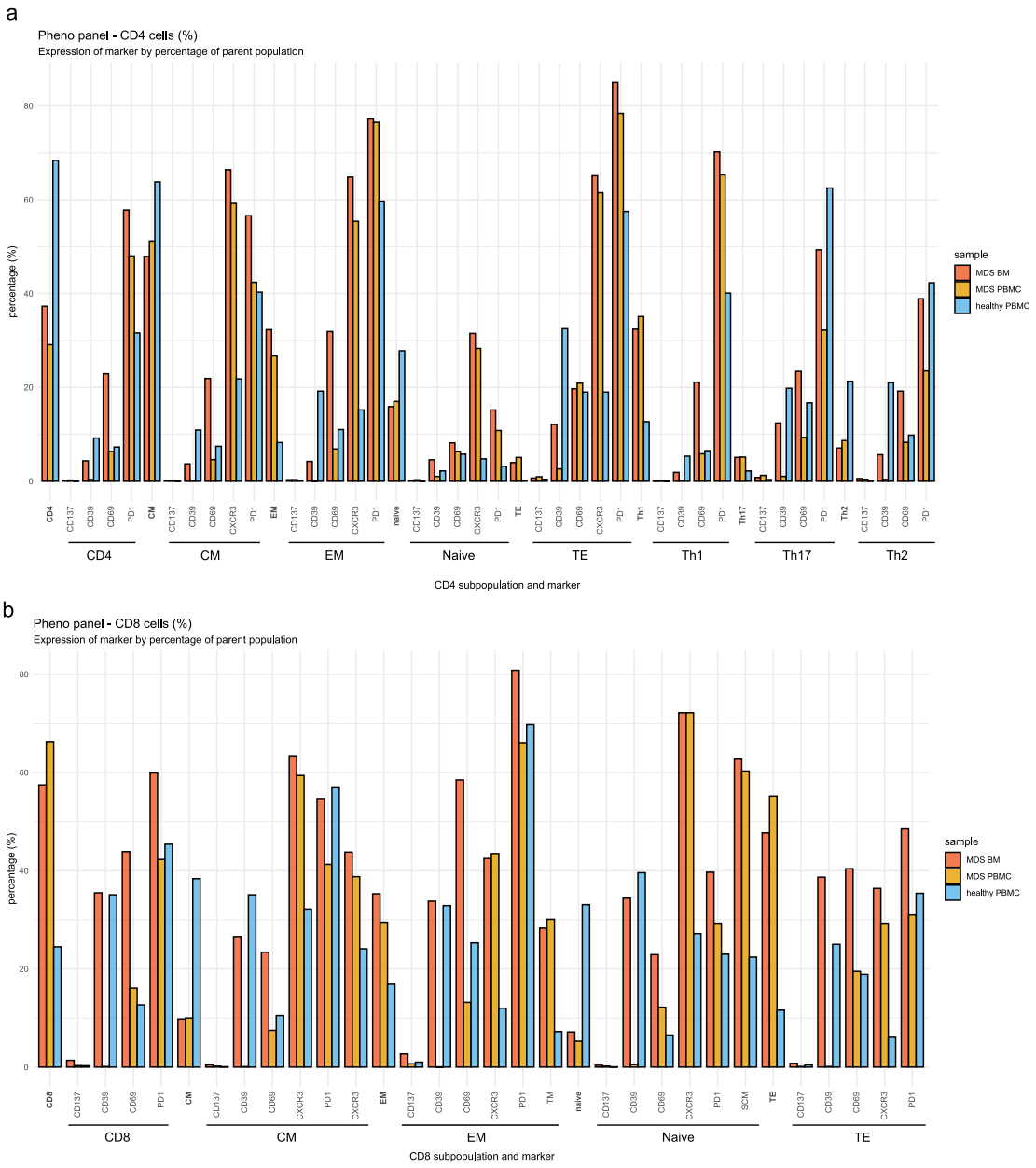

Fig. 5. Barplot showing frequency of subpopulations in (a) CD4 and (b) CD8 T cells. Expression of functional markers as expressed by percentage of positive cells relative to its parent population. Red and orange bars are bone marrow and PBMC from a patient with MDS, while blue bars are PBMC from a healthy donor. (For interpretation of the references to color in this figure legend, the reader is referred to the Web version of this article.)

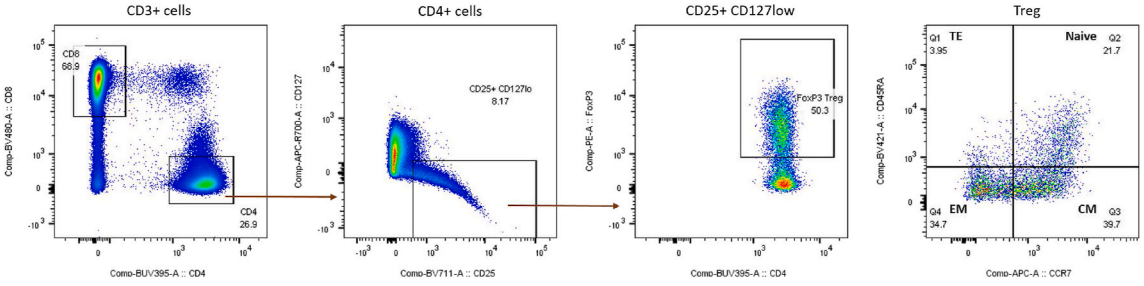

Fig. 6. Treg panel gated on PBMC from a patient with MDS. Gating steps prior to the gating of CD4 and CD8 cells are the same as in the phenotype panel. PD-1, CTLA-4, LAG-3, TIM-3 and Ki67 is measured on all subpopulations.

2.3. Regulatory T cell panel

Regulatory T cells (Treg) are important mediators of immune suppression. In cancer, Tregs are often enriched in the tumor microenvironment, and increased numbers correspond with poorer clinical outcome [21].

In the regulatory T cell panel, the frequency of Tregs was determined as CD4 cells expressing $CD25^{hi}$, $CD127^{lo}$ and $FoxP3^{+}$ (Fig. 6) [22]. FoxP3 is a transcription factor requiring permeabilization of both the cell membrane and nucleus before staining. Several functional markers were included in the panel to measure immune exhaustion and suppressive potential of the Tregs. Ki67 is strictly expressed during cell division and hence marks proliferative cells [23]. Proliferation is a hallmark for naïve and memory T cells upon meeting their antigen. PD-1,[20] CTLA-4,[20] LAG-3 [24], and TIM-3 [24] are all important inhibitory molecules associated with exhausted immune cells and suppressive immune function in cancer and autoimmune disease. Markers associated with memory and effector cells, CD45RA and CCR7, were included, as well as CD8, so that inhibitory markers could be detected on both CD4 and CD8 subsets.

In our example, where we stained bone marrow and PBMC from a patient with high-risk MDS compared with PBMC from a HD, 4% of CD4

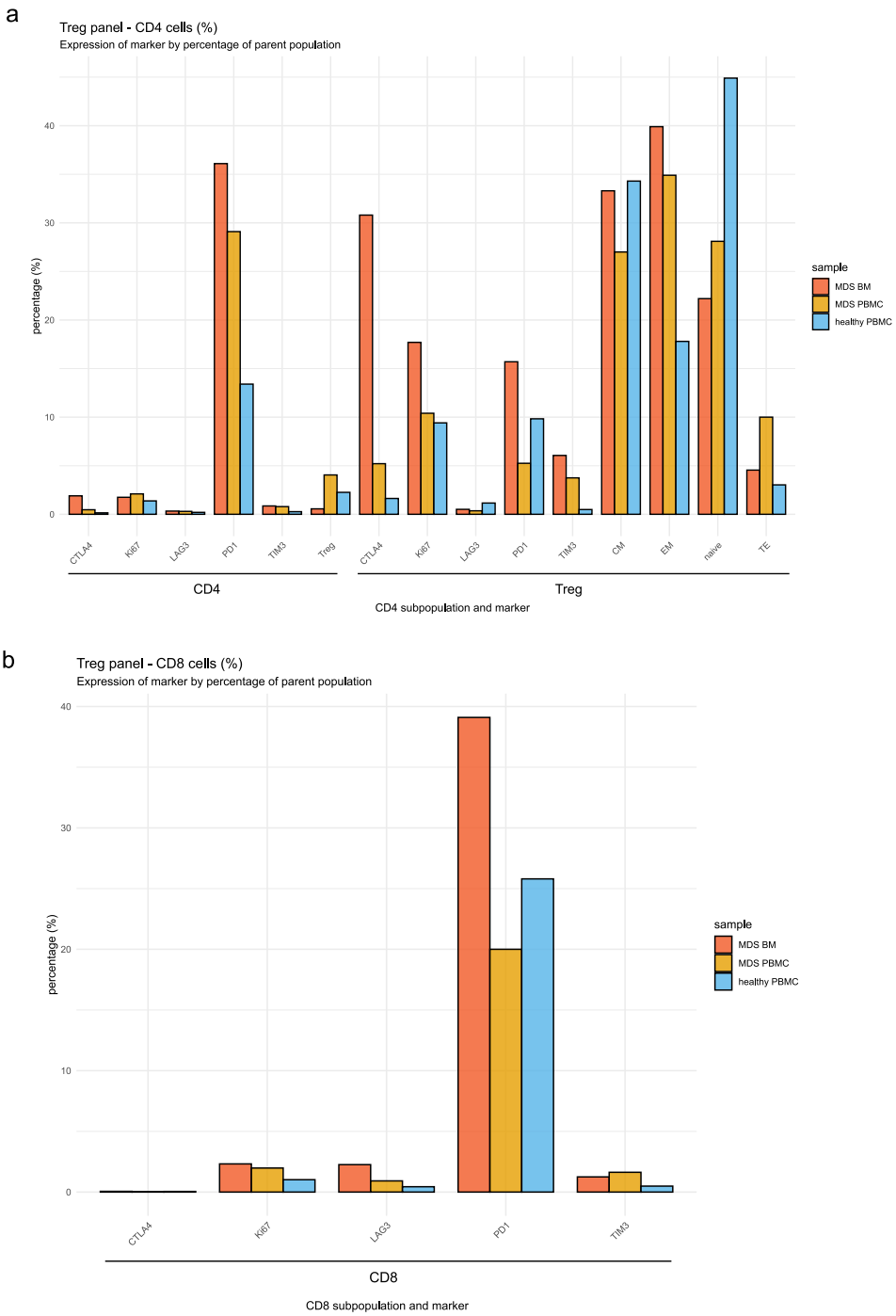

Fig. 7. Barplot showing (a) frequency of FoxP3 positive Tregs, expression of functional markers on CD4 cells and Tregs, and expression of functional markers on (b) CD8 cells. Red and orange bars are bone marrow and PBMC from a patient with MDS, while blue bars are PBMC from a healthy donor. (For interpretation of the references to color in this figure legend, the reader is referred to the Web version of this article.)

cells were Tregs in the MDS PBMC samples, compared to 2.5% in the HD, and only 0.5% in the bone marrow of the MDS patient. However, the bone marrow Tregs were more proliferative with higher Ki67 values and showed a more suppressive phenotype with higher expression of CTLA-4, PD-1, and TIM-3 (Fig. 7). The bone marrow Tregs were also less naïve compared to the PBMCs, with a predominance of EM phenotype.

2.4. Myeloid panel

In the myeloid panel, markers for distinguishing monocytes, dendritic cells (DCs), and myeloid derived suppressor cells (MDSCs) were included (Fig. 8). Monocytes and dendritic are antigen-presenting cells that prime T cells by presenting peptide fragments of tumor-associated antigens on their HLA class I and II molecules [25,26]. MDSCs, on the other hand, suppress immune responses in the tumor microenvironment and promote tumor progression [27].

The myeloid subsets are all lin$^-$ (CD3$^-$ CD19$^-$). MDSCs can either be monocytic (M-MDSC) or granulocytic (G-MDSC). M-MDSC are HLA-DR$^+$ CD11b$^+$ CD33$^{+/hi}$ CD14$^+$ CD15$^-$ and G-MDSC HLA-DR$^+$ CD11b$^+$ CD33$^{+/lo}$ CD14$^-$ CD15$^+$ [27]. DCs are all HLA-DR$^+$ and are divided into myeloid DC (mDC - CD14$^-$ CD16$^-$ CD11b$^+$ CD33$^+$ CD11c$^+$), plasmacytoid DC (pDC CD14$^-$ CD16$^-$ CD11b$^-$ CD33$^-$ CD123$^+$), and CD14$^+$ DC (CD14$^+$ CD11c$^+$) [25]. Furthermore, monocytes express CD11b and HLA-DR, and can be subdivided by their expression of CD14 and CD16. Classical monocytes are CD14^{++} CD16$^-$, intermediate CD14^{++} CD16$^+$, and non-classical monocytes CD14^{lo} CD16$^+$ [26].

PD-L1, a suppressive marker expressed on tumor cells and in the tumor microenvironment, was included and measured on the myeloid cells [20]. CD34 allowed for quantification of hematopoietic stem cells, which in MDS often is associated with malignant cells [28]. Staining of bone marrow and PBMC from a patient with MDS, compared to HD PBMC, using the myeloid panel showed 10% CD34 hematopoietic stem cells in the bone marrow of the MDS patient, compared to less than 1% in the PBMC, which is expected in this disease (Fig. 9). M-MDSCs were recorded at similar frequencies in all samples (3.5–5%), but G-MDSCs showed a higher frequency in the PBMC of the MDS patient, compared to the bone marrow sample and the HD (8% of HLA-DR negative cells in the PBMC of the MDS patient, compared to 0% in the BM sample and HD). When looking at the expression of PD-L1 on the various subpopulations, we found elevated expression in the MDS patient, especially on the classical and intermediate monocytes, in the bone marrow. It is worth noting that the percentage of PD-L1 positive cells is higher on monocytes in the bone marrow than on the CD34 positive cells since CD34 is associated with cancer stem cells in MDS, and monocytes dysplastic derives thereof. A high PD-L1 expression on monocytes has been correlated with poor survival in several malignancies [29,30].

2.5. NK panel

Natural killer (NK) cells are lymphoid innate immune cells, capable of targeting virally infected and malignant cells, that downregulates HLA-expression in order to hide from T cells [31]. While NKT cells are similar to NK cells but utilize a specialized T cells receptor to recognize lipid fragments bound to the HLA like molecule CD1d [32].

In the NK panel, we distinguished NK cells by measuring the expression of CD16 and CD56. NK cells are CD3$^-$ and CD19$^-$, and can be either CD56^{bright} CD16^{dim}, CD56^{bright} CD16$^-$, or CD56^{dim} CD16^{bright}. They were then further subtyped by whether they express other markers associated with increased cytotoxicity, such as increased CD38, CD69, CD107a, or are double positive for CD45RA and CD45RO (Fig. 10) [31]. NKT cells were stained using tetramerized CD1d molecules loaded with alpha-galactosylceramide (alpha-gal-cer), a glycolipid which invariant NKT cells specifically bind [32]. The NKT cells were then subdivided into being either CD4, CD8, or double negative. We also included an antibody for CD19 to quantify the presence of B cells.

We stained bone marrow and PBMC from a patient with MDS and PBMC from a HD with the NK panel in our example. There was a predominance of CD56^{dim} CD16^{hi} NK cells in all samples (Fig. 11), and these

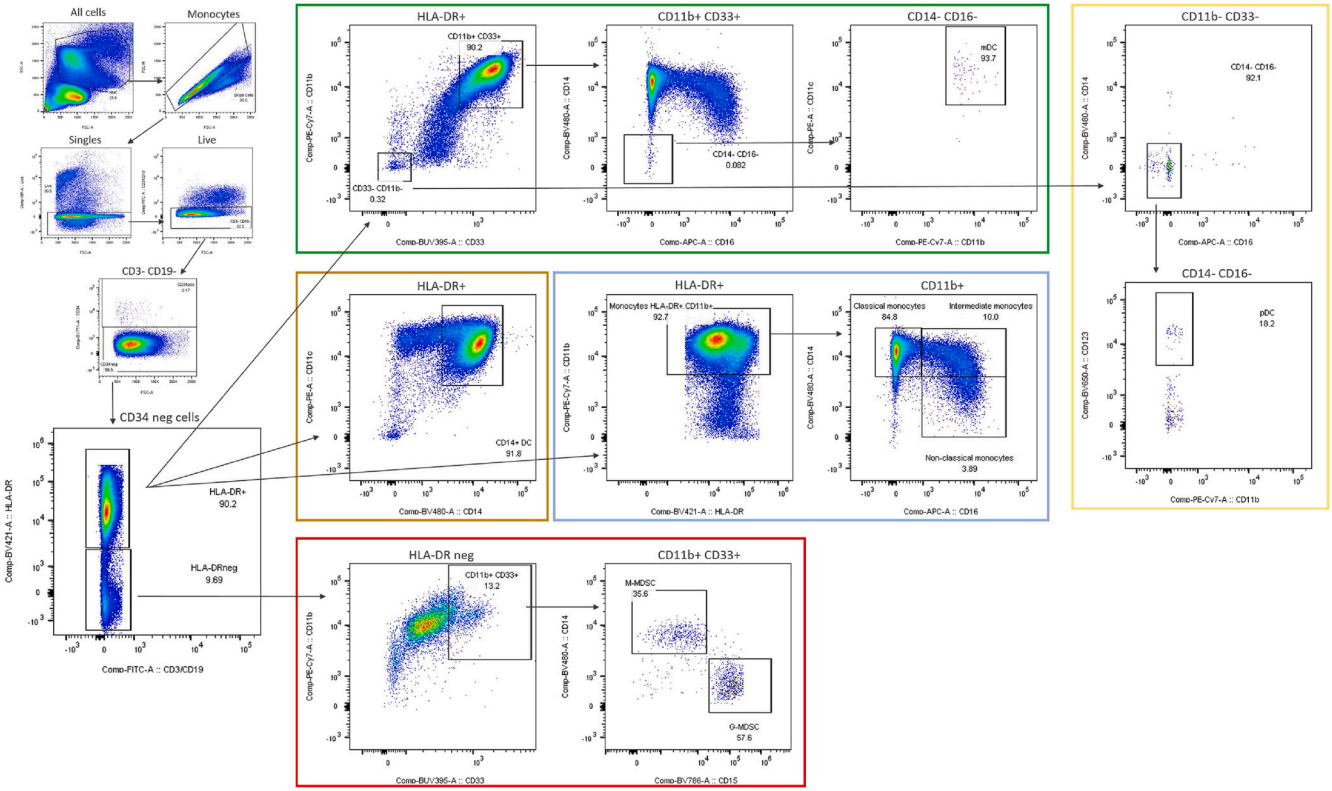

Fig. 8. Myeloid panel gated on PBMC from a patient with MDS. PD-L1 is measured on all subpopulations.

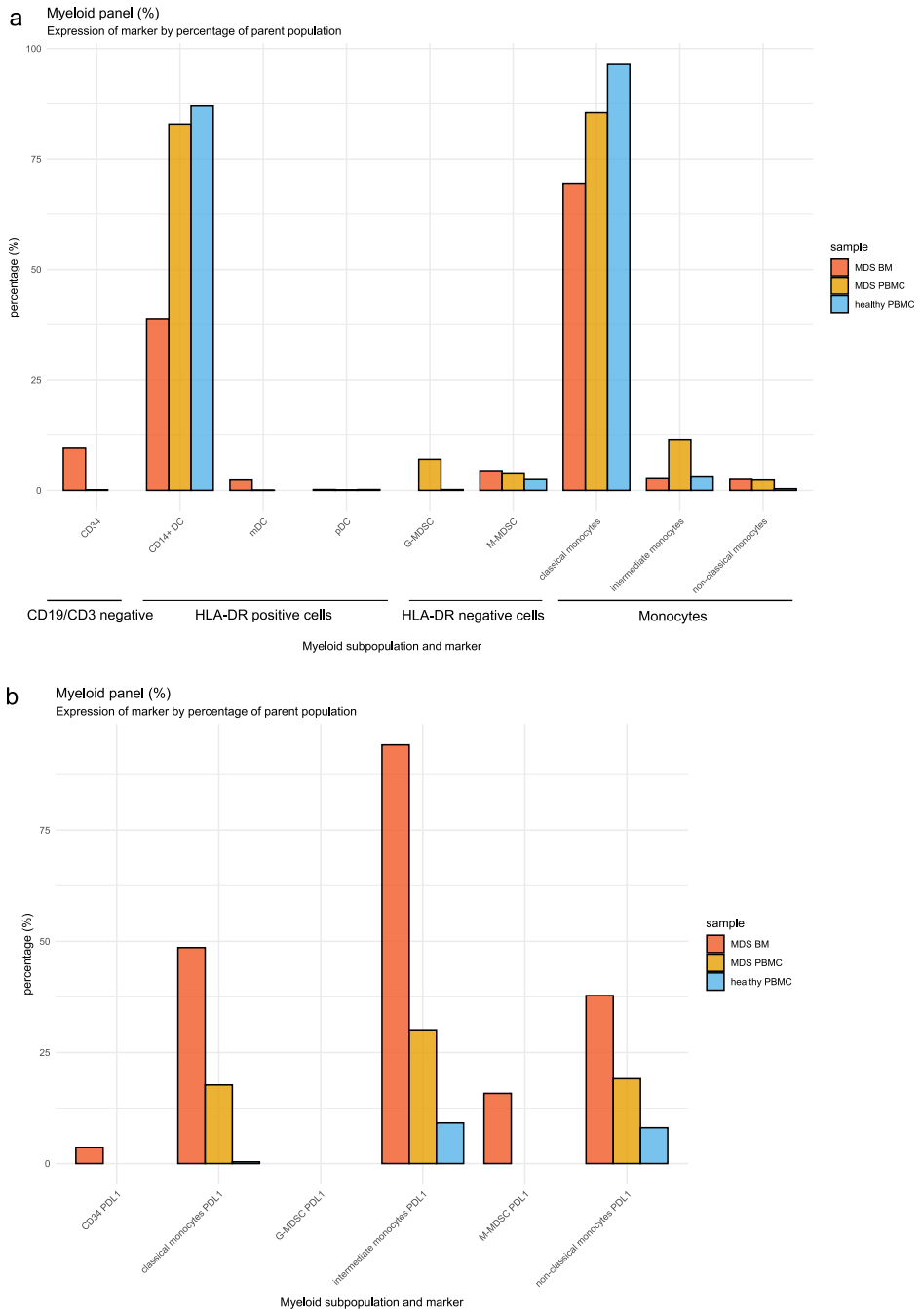

Fig. 9. Barplot showing (a) frequency of myeloid derived suppressor cells, dendritic cells, hematopoietic stem cells (CD34) and monocytes. (b) Expression of PDL1 on various myeloid cell populations. Red and orange bars are bone marrow and PBMC from a patient with MDS, while blue bars are PBMC from a healthy donor. (For interpretation of the references to color in this figure legend, the reader is referred to the Web version of this article.)

cells expressed more CD69 in the MDS patient than in the HD. Only few NK cells expressed CD107a or were double positive for CD45RA and CD45RO. NKT cells were detectable in the HD at a frequency of 0.6% of CD3 positive cells but were not present in the MDS patient.

2.6. *Explorative analysis and data visualization*

Researchers should always have a pre-determined hypothesis, or specific scientific questions, that the experiments are designed to answer. Statistical comparison of two or more groups, e.g., before vs. after treatment or responder vs. non-responder, can then be performed for either the median fluorescence intensity (MFI) of a marker to compare levels of expression or by comparing the number of positive cells in subpopulations relative to their respective parent population. The full potential of multicolor flow cytometry, however, lies in its ability to perform explorative studies, which can reveal novel subpopulations and important correlations that were unthought-of before the experiment was conducted. To detect such correlations, researchers can use unsupervised clustering together with dimensionality reduction techniques to visualize and dissect the multiparametric datasets, e.g., t-distributed stochastic neighbor embedding (t-SNE) [33] or Uniform Manifold Approximation and Projection (UMAP) [34]. In contrast to supervised clustering methods, unsupervised clustering (e.g., FlowSOM [35]) is not limited by the user's own experience with flow cytometry

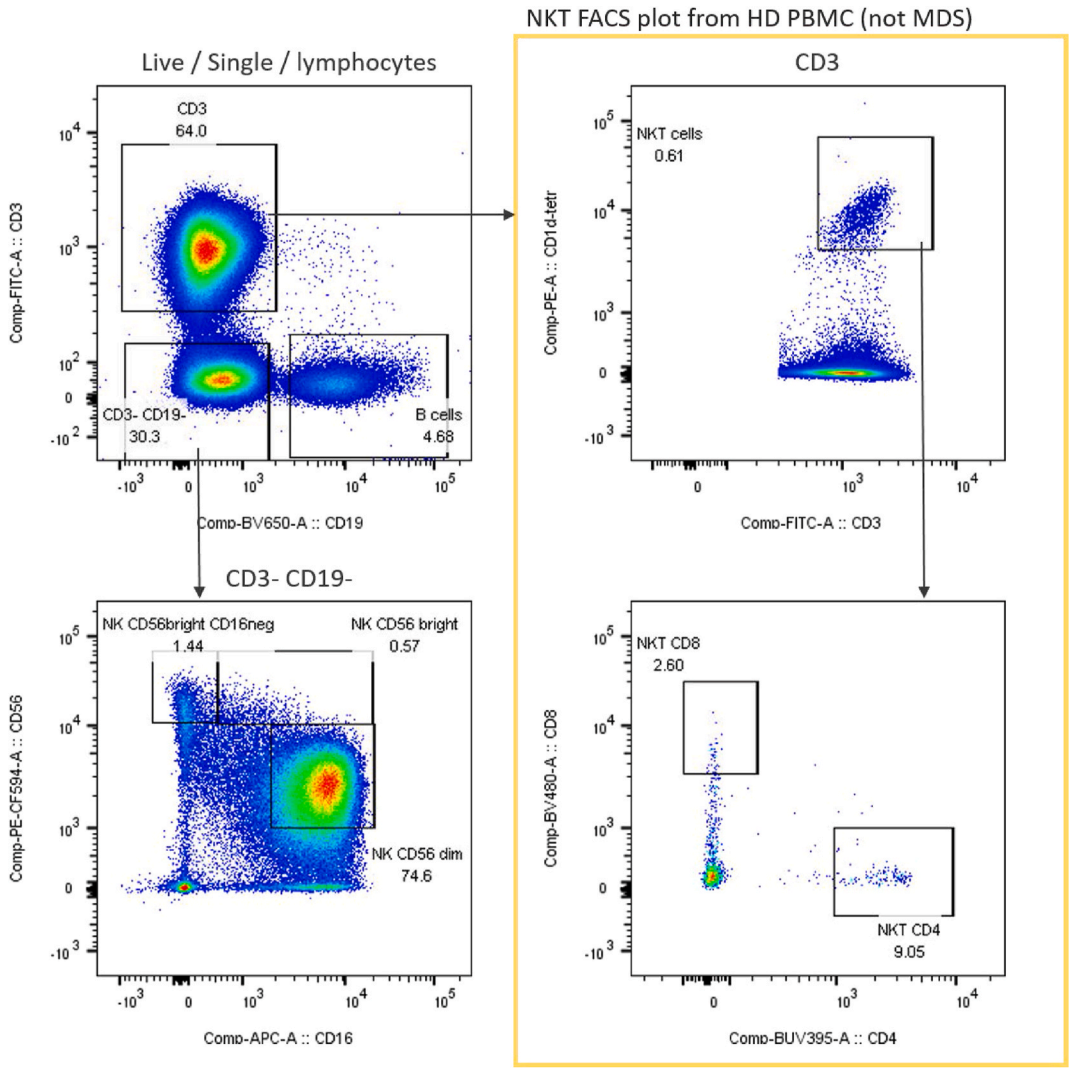

Fig. 10. NK panel gated on PBMC. Lineage gating and NK subtype plots are from a patients with MDS, while NKT plots are from a healthy donor PBMC. CD45RA CD45RO double positive cells, CD38, CD69 and CD107a is measured on all subpopulations.

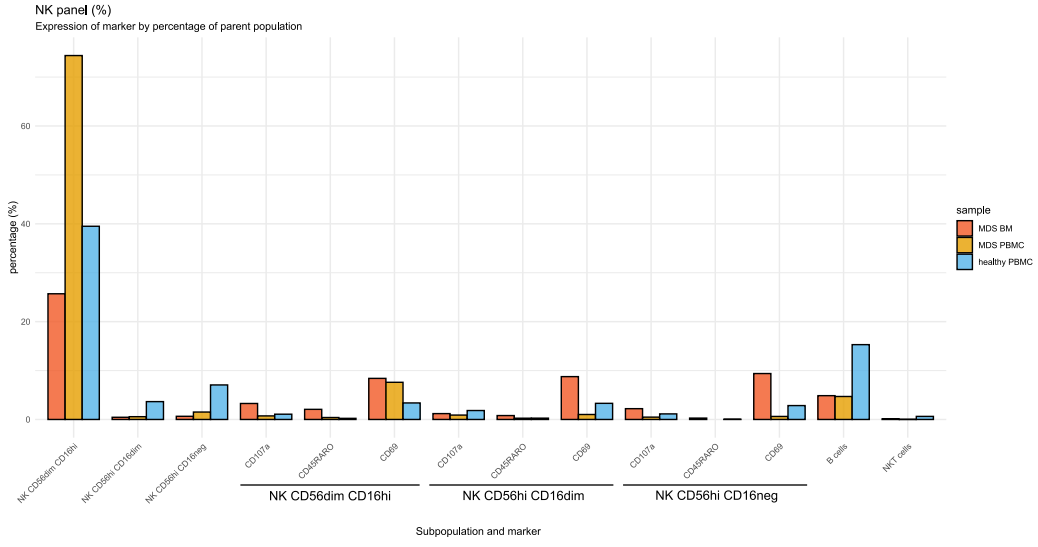

Fig. 11. Barplot showing frequency of subpopulations for NK, NKT and B cells.

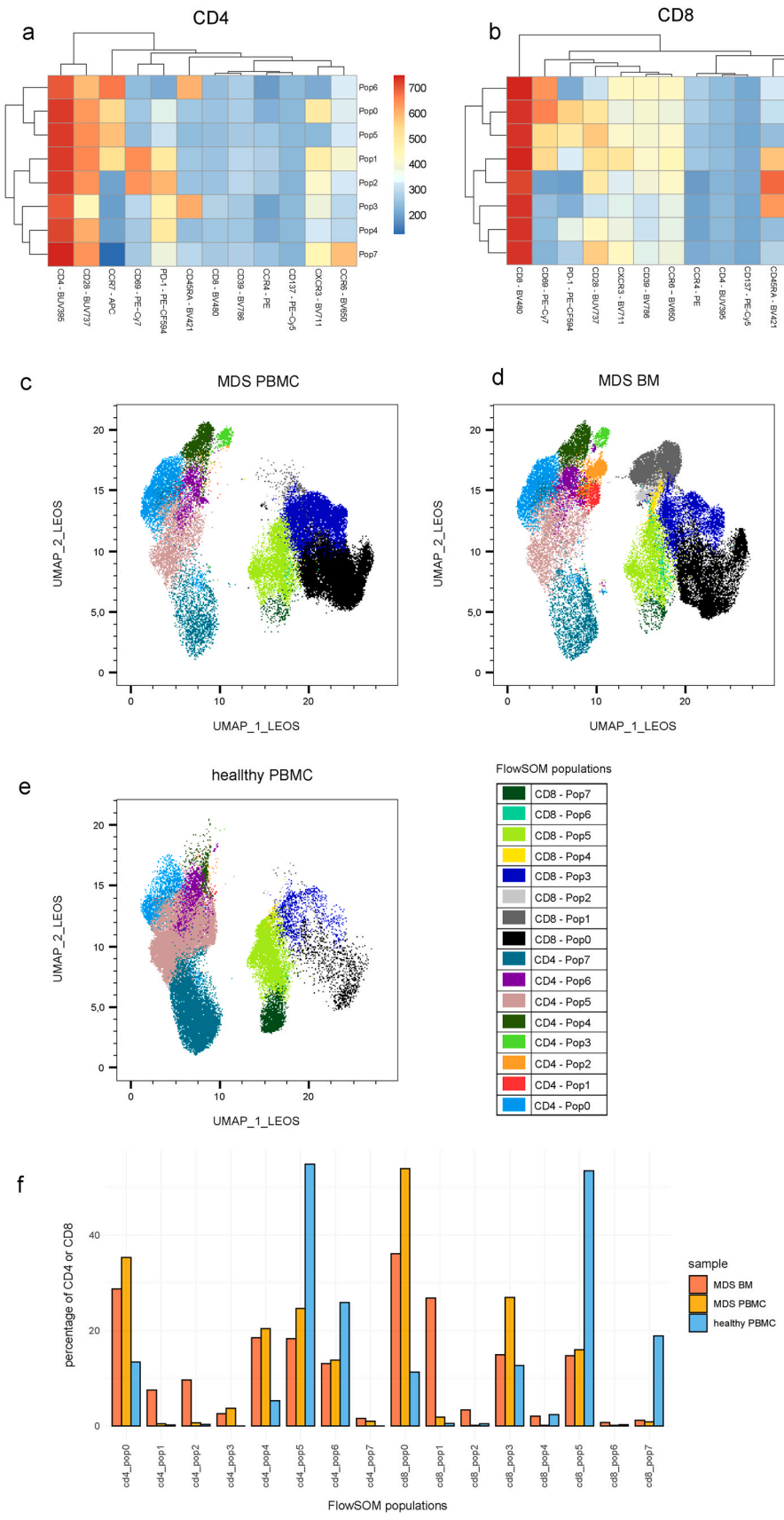

Fig. 12. Unsupervised clustering of the phenotype panel using FlowSOM on concatenated T cells in FlowJo, to detect a total of 16 subpopulations (Pop0-Pop7) on (a) CD4 cells and (b) CD8 cells. Two samples from a patient with MDS (PBMC and BM) and one PBMC sample from a healthy donor were included in the concatenation. Figure a and b show heat map (FlowSOM plugin output) of the relative fluorescent intensity for the markers associated with the identified CD4 and CD8 subpopulations. Dimensionality reduction was then performed using UMAP on the concatenated cells to visually inspect differences in density of clusters among (c) PBMC and (d) BM from an MDS patient, and (e) PBMC from a healthy donor. The identified CD4 and CD8 subpopulations from the FlowSOM analysis, were then overlaid the UMAP visualizations to create an overview of their prevalence in the three samples. Colors of clusters represent the subpopulations seen in figure a and b. Figure f is showing frequency, as percentage of CD4 or CD8 cells, of the identified CD4 and CD8 subpopulations from the FlowSOM analysis. Red and orange bars are the MDS bone marrow and PBMC samples, while blue bars are healthy donor PBMC. (For interpretation of the references to color in this figure legend, the reader is referred to the Web version of this article.)

gating and theoretical knowledge of how cell subtypes are defined [36].

We performed unsupervised clustering on the two MDS samples and a healthy donor (Fig. 12) using the FlowSOM [35] plugin in FlowJo. For the phenotype panel, the three samples were concatenated (data aggregated into one file) on their respective CD3 gate, and FlowSOM run using the default settings with 8 clusters for both CD4 and CD8 cells. UMAP was used to create clustering maps for the three samples, where the FlowSOM populations could be superimposed, generating a visual overview of all identified CD4 and CD8 clusters and their dominance in each sample.

The clustering method identified that in the CD8 compartment, TE cells (CD45RA + CCR7-) and EM cells (CD45RA- CCR7-) were more frequent in the MDS patient, while naïve (CD45RA + CCR7+) and CM cells (CD45RA- CCR7+) were less frequent compared to the HD, which corresponds to the findings based on our manual gating. It also identified a CD8 EM population (CD8-pop1) that was high in both CD69 and PD-1. This double-positive subpopulation accounted for 24% of CD8 cells in the MDS bone marrow sample, but only 1–2% in the two PBMC samples, which was overlooked using the manual gating. In the CD4 compartment, CM and EM cells double-positive for CD69 and PD-1 (CD4-pop1 and CD4-pop2) were more dominant in the BM sample compared to the two PBMC samples. Similar unsupervised clustering analyses for the Treg, myeloid, and NK panels are shown in supplementary figures 2-4.

3. Discussion

We have presented four flow cytometry panels for analyzing immune cell compartments and a workflow for constructing new panels. Multicolor flow cytometry is a powerful tool since substantial multiparametric data can be collected for each cell (event), generating large amounts of data from each experiment. However, flow cytometry is prone to technical errors, spectral overlap, and subjective data interpretation, which can create biases in the data analyses. Furthermore, limitations, such as inter-experiment variability and poor data resolution when many colors are used simultaneously, should be addressed. If the researcher applies a systematic workflow for pairing colors to markers, optimized for the equipment intended to run the experiments (e.g., generating a SSM to guide color selection), many limitations can be overcome. We also address quality control methods, titration of antibodies, compensation, and staining of cells for obtaining optimal results. To handle the vast amount of data generated by multicolor flow cytometry, unsupervised clustering techniques are valuable tools for identifying significant subpopulations of immune cells while avoiding gating bias.

4. Materials and methods

4.1. FACS machine configuration

LSR Fortessa from BD bioscience (Franklin Lakes, NJ, USA) with a five laser setup (consisting of 488 nm blue, 460 nm red, 532 nm green, 405 nm violet, and 355 nm UV). See supplementary figure 1 for filter configuration. The SSM was calculated in FlowJo v10 software after acquiring single stained compensation beads for all the colors available for the laser setup and filter configuration on our FACS machine.

4.2. Staining cells

First, antibody-mixtures for each of the panels were made in advance and stored dark at 4 °C. To make the antibody-mixture, the volumes of each antibody selected from previous antibody titration experiments were added to a tube, times the number of samples needed to be stained. An additional 50 μl of BD brilliant stain buffer (BD; 566349) was added per sample, and lastly, the mixture was topped up with PBS to reach a total volume of 85 μl/sample. Near-IR viability dye (Thermo Fisher Invitrogen™; L34975) and CD1d tetramers (Tetramer Shop; HCD1d-001) were not added to the master-mixtures but added separately to the cells when staining. In the T regulatory panel, only surface markers were added to the mixtures. Intracellular markers (FoxP3 and Ki67) were added later in the process when cells had been fixed and permeabilized.

We thawed PBMC and bone marrow cells in 37° RPMI 1640 (Thermo Fisher, Gibco), with 10% fetal calf serum (Thermo Fisher, Gibco) added. After thawing, the cells were incubated for 10 min in 10% human serum (Sigma Aldrich) to saturate FC-receptors on cells and minimize unspecific binding of antibodies, which is of particular importance if staining myeloid cells. Afterward, cells were counted and split into four 96-well plates, with approximately one to five million cells per staining, and washed twice in FACS buffer (PBS + 2% fetal calf serum). Next, the supernatant was removed, leaving approximately 15 μl of cells in each well. Cells were stained by adding 85 μl of the antibody-mixture to each well. NIR was then added to all samples and CD1d tetramers to the cells stained with the NK/NKT panel. All wells were mixed, and cells were incubated for 30 min on ice. After incubation, cells were washed twice with FACS buffer and then fixed with 1% PFA or acquired immediately at the FACS machine. The cells stained with the T regulatory panel were fixed and permeabilized using BD TF permeabilization kit (BD Pharmingen; 562574), after which the intracellular antibodies were added to the cells. Following 30 min of incubation and washing with perm/wash buffer, the cells were resuspended in FACS buffer and ready for analysis.

When the phenotype panel was combined with ICS for analyzing T cells that produce cytokines when presented to specific antigens, the thawed cells were first stimulated for 12 h in media containing the peptides of interest at a concentration of 1 μg/ml, Brefeldin A (BD GolgiPlug, 555029), and 5% human serum. During stimulation, a CD107a antibody (Biolegend, 328640) was added to detect degranulation. Following stimulation and washing steps, the cells were stained with all markers from the phenotype panel, except CXCR3, CCR4, and CCR6, and then fixed and permeabilized using BD Fixation/Permeabilization kit (BD Cytofix/Cytoperm; 554714). After permeabilization, the cells were stained with antibodies that bind intracellular interferon gamma (BD, 562016) and tumor necrosis factor alpha (BD, 563418), and then analyzed in the FACS machine.

For combining phenotyping with MHC tetramer staining, to characterize T cells that bind to specific antigens, the thawed cells were first stained with tetramerized MHC-molecules loaded with the specific peptides of interest and tagged with fluorescent molecules. The antibodies for the phenotype panel, except CXCR3, CCR4, and CCR6, were then added to the cells.

Ethics

All samples used for this study were analyzed following oral and written consent from the patient.

Funding

Financial support to this study was provided by the Danish Cancer Society, grant no. R72-A4531 and R146-A9531-16-S2, and Herlev-Gentofte hospital research grant.

Declaration of competing interest

None.

Appendix A. Supplementary data

Supplementary data to this article can be found online at https://doi.org/10.1016/j.ab.2021.114210.

References

[1] S. Sanjabi, S. Lear, New cytometry tools for immune monitoring during cancer immunotherapy, Cytometry B Clin. Cytometry 1 (2021).
[2] M. Büscher, Flow cytometry instrumentation – an overview, Current Protocols in Cytometry 87 (2019) e52.
[3] L.A. Herzenberg, et al., The history and future of the fluorescence activated cell sorter and flow cytometry: a view from stanford, Clin. Chem. 48 (2002) 1819–1827.
[4] H.T. Maecker, J.P. McCoy, A model for harmonizing flow cytometry in clinical trials, Nat. Immunol. 11 (2010) 975–978.
[5] R. Nguyen, S. Perfetto, Y.D. Mahnke, P. Chattopadhyay, M. Roederer, Quantifying spillover spreading for comparing instrument performance and aiding in multicolor panel design, Cytometry 83A (2013) 306–315.
[6] J.G. Burel, et al., An integrated workflow to assess technical and biological variability of cell population frequencies in human peripheral blood by flow cytometry, J.I. 198 (2017) 1748–1758.
[7] L. Wang, R.A. Hoffman, Standardization, calibration, and control in flow cytometry, Current Protocols in Cytometry 79 (2017).
[8] A. Cossarizza, et al., Guidelines for the use of flow cytometry and cell sorting in immunological studies (second edition), Eur. J. Immunol. 49 (2019) 1457–1973.
[9] der Strate, B. van, et al., Best practices in performing flow cytometry in a regulated environment: feedback from experience within the European Bioanalysis Forum, Bioanalysis 9 (2017) 1253–1264.
[10] N. Selliah, et al., Flow cytometry method validation protocols, Curr Protoc Cytom 87 (2019) e53.
[11] D.S. Chen, I. Mellman, Oncology meets immunology: the cancer-immunity cycle, Immunity 39 (2013) 1–10.
[12] Y.D. Mahnke, T.M. Brodie, F. Sallusto, M. Roederer, E. Lugli, The who's who of T-cell differentiation: human memory T-cell subsets, Eur. J. Immunol. 43 (2013) 2797–2809.
[13] L. Gattinoni, D.E. Speiser, M. Lichterfeld, C. Bonini, T memory stem cells in health and disease, Nat. Med. 23 (2017) 18–27.
[14] F. Sallusto, A. Lanzavecchia, Heterogeneity of CD4+ memory T cells: functional modules for tailored immunity, Eur. J. Immunol. 39 (2009) 2076–2082.
[15] K.E. Kortekaas, et al., CD39 identifies the CD4+ tumor-specific T cell population in human cancer, *Cancer Immunol Res* canimm (2020), https://doi.org/10.1158/2326-6066.CIR-20-0270, 0270.2020.
[16] Y. Simoni, et al., Bystander CD8+ T cells are abundant and phenotypically distinct in human tumour infiltrates, Nature 557 (2018) 1.
[17] Y. Mita, et al., Crucial role of CD69 in anti-tumor immunity through regulating the exhaustion of tumor-infiltrating T cells, Int. Immunol. 30 (2018) 559–567.
[18] D. Cibrián, F. Sánchez-Madrid, CD69: from activation marker to metabolic gatekeeper, Eur. J. Immunol. 47 (2017) 946–953.
[19] Q. Ye, et al., CD137 accurately identifies and enriches for naturally occurring tumor-reactive T cells in tumor, Clin. Canc. Res. 20 (2014) 44–55.
[20] A. Ribas, J.D. Wolchok, Cancer immunotherapy using checkpoint blockade, Science 359 (2018) 1350–1355.
[21] M. Najafi, B. Farhood, K. Mortezaee, Contribution of regulatory T cells to cancer: a review, J. Cell. Physiol. 234 (2019) 7983–7993.
[22] A. Tanaka, S. Sakaguchi, Regulatory T cells in cancer immunotherapy, Cell Res. 27 (2016) 1–7.
[23] A. Soares, et al., Novel application of Ki67 to quantify antigen-specific in vitro lymphoproliferation, J. Immunol. Methods 362 (2010) 43–50.
[24] A.C. Anderson, N. Joller, V.K. Kuchroo, Lag-3, tim-3, and TIGIT: Co-inhibitory receptors with specialized functions in immune regulation, Immunity 44 (2016) 989–1004.
[25] M. Collin, N. McGovern, M. Haniffa, Human dendritic cell subsets, Immunology 140 (2013) 22–30.
[26] L. Ziegler-Heitbrock, et al., Nomenclature of monocytes and dendritic cells in blood, Blood 116 (2010) e74–e80.
[27] V. Bronte, et al., Recommendations for myeloid-derived suppressor cell nomenclature and characterization standards, Nat. Commun. 7 (2016) 1–10.
[28] C.Y. Ok, K.H. Young, Checkpoint inhibitors in hematological malignancies, J. Hematol. Oncol. 10 (2017) 103.
[29] H. Yasuoka, et al., Increased both PD–L1 and PD–L2 expressions on monocytes of patients with hepatocellular carcinoma was associated with a poor prognosis, Sci. Rep. 10 (2020) 10377.
[30] X. Zhang, et al., Expression of PD-L1 on monocytes is a novel predictor of prognosis in natural killer/T-cell lymphoma, Front. Oncol. 10 (2020).
[31] E. Krzywinska, et al., Identification of anti-tumor cells carrying natural killer (NK) cell antigens in patients with hematological cancers, EBioMedicine 2 (2015) 1364–1376.
[32] S. Nair, M.V. Dhodapkar, Natural killer T cells in cancer immunotherapy, Front. Immunol. 8 (2017).
[33] L. van der Maaten, G. Hinton, Visualizing Data using t-SNE, J. Mach. Learn. Res. 9 (2008) 2579–2605.
[34] L. McInnes, J. Healy, J.U.M.A.P. Melville, Uniform Manifold Approximation and Projection for Dimension Reduction, 2018 arXiv:1802.03426 [cs, stat].
[35] S.V. Gassen, et al., FlowSOM: using self-organizing maps for visualization and interpretation of cytometry data, Cytometry 87 (2015) 636–645.
[36] P. Liu, et al., Recent advances in computer-assisted algorithms for cell subtype identification of cytometry data, Front Cell Dev Biol 8 (2020).